MULTI-AXIS MANEUVER DESIGN FOR AIRCRAFT PARAMETER ESTIMATION

Mathias Stefan Roeser, Institute of Flight Systems
DLR (German Aerospace Center)
Lilienthalplatz 7, 38108 Braunschweig, Germany

Abstract

A flight test campaign for system identification is a time and cost consuming task. Models derived from wind tunnel experiments and CFD calculations must be validated and/or updated with flight data in order to match the real aircraft stability and control characteristics. Classical maneuvers for system identification are mostly one-surface-at-time inputs and need to be performed several times at each flight condition. Multi-surface or multi-axis maneuvers have been designed in the past, however, they are only time or frequency decorrelated. Therefore, a new design method based on the wavelet transform was developed that allows to define multi-axis inputs in the time-frequency domain. Using such inputs, simulated flight test data was generated from a high-quality Airbus A320 dynamic model. System identification was then performed with this data and the results show that accurate aerodynamic parameters can be extracted from these multi-axis maneuvers.

NOMENCLATURE

Symbols

2^{N_f}	frequency tiling
2^{N_t}	time tiling
A	dilation parameter
b	wing span, m
B	translation parameter
$\bar{c}$	mean aerodynamic chord, m
C_D	drag coefficient
C_L	lift coefficient
C_l, C_m, C_n	body-axes nondimensional moment coefficients
C_X, C_Y, C_Z	body-axes nondimensional force coefficients
e	Oswald factor
E	energy spectrum
g	acceleration due to gravity, m/s^2
i_{HT}	horizontal tail deflection, deg
I_x, I_y, I_z, I_{xz}	mass moments of inertia, Nm^2
k_1	linear drag polar parameter
m	aircraft mass, kg
p, q, r	body-fixed rotational rates, deg/s
p^*, q^*, r^*	normalized body-fixed rotational rates
$\bar{q}$	dynamic pressure, N/m^2
S	wing reference area, m^2
S_{HT}	horizontal tail reference area, m^2
t	time, s
Δt	time step for multistep input, s
T	engine thrust, N
$T(A, B)$	wavelet transform

u, v, w	body-fixed translational velocities, m/s
V	true airspeed, m/s
$x(t)$	continuous signal
x_{HT}, z_{HT}	horizontal tail lever arms, m
x'_{HT}	distance between horizontal tail neutral point and wing-body center of gravity, m

Greek Symbols

α	angle of attack, deg
α_{dyn}	dynamic angle of attack at HT, deg
β	angle of sideslip, deg
$\delta\varepsilon/\delta\alpha$	downwash change due to change of angle of attack
ε_{HT}	downwash angle at HT, deg
η	elevator deflection, deg
Λ	wing aspect ratio
ω	frequency, 1/s
ϕ, θ	roll and pitch attitude, deg
$\psi_{(A,B)}(t)$	normalized wavelet function
τ	time delay, s
ξ_l, ξ_r	left/right aileron deflection, deg
ζ	rudder deflection, deg

Subscripts

0	initial or reference value
HT	horizontal tail
WB	wing body

Abbreviations

CFD	Computational Fluid Dynamics
CWT	Continuous Wavelet Transform
DWPT	Discrete Wavelet Packet Transform
DWT	Discrete Wavelet Transform
FFT	Fast Fourier Transform
IDWPT	Inverse Discrete Wavelet Packet Transform
QTG	Qualification Test Guide
Sys-ID	System Identification
TFP	Time-Frequency Plane
TFR	Time-Frequency Representation
WPT	Wavelet Packet Transform

1 INTRODUCTION

Aerodynamic models used for certification, performance and handling qualities evaluations, flight simulators, control law design, etc., must be validated and perhaps updated with flight test data to match the real aircraft stability and control characteristics. For this purpose an extensive system identification flight test campaign is usually performed, in which dedicated maneuvers are conducted at distinct pre-defined flight conditions.

Maneuver design for aircraft parameter estimation is done using an *a-priori* model of the aircraft, typically derived from wind tunnel experiments and CFD calculations. It is common practice to create inputs that excite the aircraft at its expected eigenmodes. Marchand [1, 2] und Plaetschke et al. [3] showed that evaluating the frequency response magnitude of the terms of each equation of the aircraft's linear system is one possibility to identify the regions of identifiability of each derivative. These regions lie in the vicinity of the natural frequencies of the aircraft's eigenmodes. However, *a-priori* aircraft models are subject to uncertainties and therefore the maneuver design must also consider frequencies slightly above and below the expected eigenfrequencies.

Classical maneuvers to excite the aircraft at its expected eigenmodes are multistep inputs. Herein the length of the steps is chosen such that the natural frequency of the excited mode lies in the center or upper third of the input spectrum [4]. Multistep inputs like doublets or 3211 signals are easy to execute manually and are therefore widely used for system identification purposes.

The 3211-input e.g. has a broad frequency spectrum, see Figure 1, and suits well for parameter estimation maneuvers, because even if the natural frequency of the aircraft response slightly changes due to different flight conditions or deviations from the *a-priori* model, this input covers these uncertainties and must not be redesigned for every flight condition. The aircraft response to these multistep inputs is also easy to interpret, which is important when identifying the model structure, as will be discussed in Section 6.

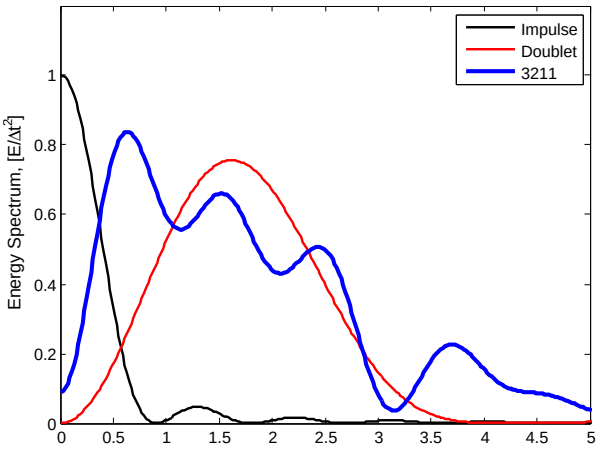

Figure 1: Frequency spectrum comparison of different standard inputs

Another type of input for system identification are frequency sweeps. However, this method is time consuming because each surface has to be excited separately and the excitation may last up to 2 minutes. The advantage is that a complete frequency response of the system to one single control input can be evaluated from a single flight test point.

Using maneuvers that excite multiple control surfaces at the same time has a great potential to reduce flight test time and costs. Such multi-axis maneuvers were already investigated in the late 70's, where Ramachandran and Wells [5] investigated the identification of aerodynamic parameters for a light aircraft by applying inputs on rudder and aileron simultaneously to minimize the correlation between the model parameters during identification. Further multi-axis maneuvers have been designed to excite the aircraft in all six-degrees of freedom.

Morelli introduced a method to create multi-axis input signals based on orthogonal optimized multi-sine waves that cover a broad range of frequencies [6, 7]. Accurate parameter estimates using the equation error method in the frequency domain were obtained from flight test data with this type of inputs applied continuously during the maneuvers.

Another approach for multi-axis maneuver design has been developed by Lichota [8]. This design method generates a so called D-Optimal signal, based on the Fisher information matrix. This method relies also on *a-priori* knowledge of the aircraft model, and is only optimal for the flight test point considered. The *a-priori* model is assumed to be linear and there is no time information about the frequencies excited.

The goal of this research is to propose new ways to design maneuvers in order to reduce flight test time to get very accurate airplane simulation models. These simulation models must at least fulfill the Qualification Test Guide (QTG) criteria for level-D full flight simulators.

A method is desired that allows to generate multi-axis input signals with the ability to specify both the frequency content and the times when the frequencies are excited, with as little parameters as possible. A parametrization is performed using the wavelet transform which has been applied for image processing, seismic signal denoising and analysis of diverse other physical phenomena [9]. The wavelet transform yields a Time-Frequency Representation (TFR) of a signal and the signal can be reconstructed from its TFR.

The idea behind the proposed method is to start by specifying the desired TFR and to generate the input signals by inverse wavelet transform.

This work is structured as follows: the next Section gives a short overview over the applied rigid-body equations of motion and the aerodynamic model. Section 3 introduces the wavelet transform and the method used for the signal definition is explained in Section 4 together with its applicability to multi-axis signals. In Section 5 parameter estimation results are presented that were obtained from simulated flight test data using the new signal generation method. A comparative discussion to already existing multi-axis maneuver designs is given in Section 6. Finally, Section 7 sums up the work in this paper giving the next steps and future applicability for the method introduced.

2 BASIC MODEL FORMULATION

The basic aircraft equations of motion are described by a six degree-of-freedom kinematic model. The translation motion is given by

$$\begin{aligned}\dot{u} &= rv - qw + \frac{\bar{q}S}{m}C_X - g\sin\theta + \frac{T}{m}\\ \dot{v} &= pw - ru + \frac{\bar{q}S}{m}C_Y + g\cos\theta\sin\phi\\ \dot{w} &= qu - pv + \frac{\bar{q}S}{m}C_Z + g\cos\theta\cos\phi\end{aligned} \tag{1}$$

and the rotational motion is given by

$$\begin{aligned}\dot{p}I_x - \dot{r}I_{xz} &= \bar{q}SbC_l - qr(I_z - I_y) + qpI_{xz}\\ \dot{q}I_y &= \bar{q}S\bar{c}C_m - pr(I_x - I_z)\\ &\quad - (p^2 - r^2)I_{xz}\\ \dot{r}I_z - \dot{p}I_{xz} &= \bar{q}SbC_n - pq(I_y - I_x) - qrI_{xz}\end{aligned} \tag{2}$$

The complete set of the aerodynamic equations follows the model in [10]. The coefficients of the aerodynamic forces and moments for the lateral-directional dynamics (C_Y, C_l, C_n) are derived by simple Taylor series expansion.

$$\begin{aligned}C_Y &= C_{Y_0} + C_{Y_\beta}\beta + C_{Y_\zeta}\zeta + C_{Y_p}p^* + C_{Y_r}r^*\\ C_l &= C_{l_0} + C_{l_\beta}\beta + C_{l_\zeta}\zeta + C_{l_p}p^* + C_{l_r}r^*\\ &\quad + C_{l_\xi}\frac{1}{2}(\xi_r - \xi_l)\\ C_n &= C_{n_0} + C_{n_\beta}\beta + C_{n_\zeta}\zeta + C_{n_p}p^* + C_{n_r}r^*\end{aligned} \tag{3}$$

with $\quad p^* = \dfrac{pbV}{2} \qquad r^* = \dfrac{rbV}{2}$

where p^* and r^* are the normalized roll and yaw rates.

The equations for the longitudinal motion are based on the two-point model described in [11]. This model separates the wing and horizontal tail influences and allows to account for the downwash lag effect of the wing to the horizontal tail.

The lift coefficient is separated into a wing-body component and a component for the horizontal tail. The drag coefficient is calculated via the simple polar equation. The pitching moment coefficient is also separated into a wing-body component and a component calculated via the body-axis components $C_{X_{HT}}$ and $C_{Z_{HT}}$ and the respective lever-arms.

$$\begin{aligned}C_L &= C_{L_{WB}} + C_{L_{HT}}\frac{S_{HT}}{S}\cos(\alpha_{dyn} - \varepsilon_{HT})\\ C_D &= C_{D_0} + k_1 C_L + \frac{C_L^2}{e\pi\Lambda}\\ C_m &= C_{m_{WB}} + C_{Z_{HT}}\frac{S_{HT}}{S}\frac{x_{HT}}{\bar{c}}\\ &\quad - C_{X_{HT}}\frac{S_{HT}}{S}\frac{z_{HT}}{\bar{c}}\end{aligned} \tag{4}$$

The separated influences of wing and tail for the longitudinal motion are calculated by

$$\begin{aligned}C_{L_{WB}} &= C_{L_0} + C_{L_{\alpha,WB}}\alpha + C_{L_{q,WB}}q^*\\ C_{L_{HT}} &= C_{L_{0,HT}} + C_{L_{\alpha,HT}}\alpha_{HT} + C_{L_{\eta,HT}}\eta\\ C_{m_{WB}} &= C_{m_{0,WB}} + C_{m_{q,WB}}q^*\end{aligned}$$

$$\begin{aligned}\alpha_{HT} &= \alpha + i_{HT} - \varepsilon_{HT} + \alpha_{dyn}\\ \alpha_{dyn} &= \tan^{-1}(qx'_{HT}/V)\\ \varepsilon_{HT} &= \varepsilon_{0,HT} + \frac{\delta\varepsilon}{\delta\alpha}\alpha(t-\tau)\end{aligned} \tag{5}$$

$$\begin{aligned}C_{X_{HT}} &= C_{L_{HT}}\sin(\alpha_{HT} - i_{HT})\\ C_{Z_{HT}} &= -C_{L_{HT}}\cos(\alpha_{HT} - i_{HT})\end{aligned}$$

with $\quad q^* = q\bar{c}V$

where q^* is the normalized pitch rate. The parameter τ represents the downwash lag effect of the wing to the horizontal tail.

The body-axis force coefficients C_X and C_Z from Equations (1) are finally derived from the lift and drag coefficient by

$$\begin{aligned}C_X &= -C_D\cos\alpha + C_L\sin\alpha\\ C_Z &= -C_L\cos\alpha - C_D\sin\alpha\end{aligned} \tag{6}$$

3 WAVELET TRANSFORM

The wavelet transform is being used for the analysis of diverse physical phenomena, e.g. in the denoising of seismic signal, climate analysis, heart monitoring, amongst others [9]. The complete wavelet transform theory goes far beyond the scope of this paper and will not be described in detail. A few essentials are provided to give

the reader some insight into the transform applied in the method. More details can be found in [9, 12, 13].

In a simple manner, the wavelet transform is a convolution of a signal to be analyzed with a wavelet function, also known as *wavelet*. The wavelet is a small wave-like function that begins and ends at zero amplitude. Some commonly used wavelets are depicted in Figure 2.

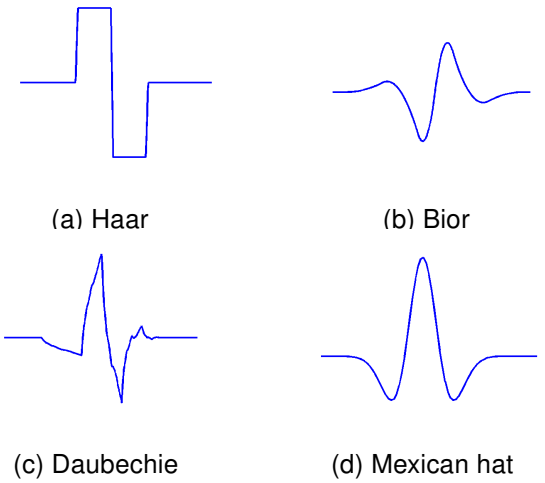

Figure 2: Wavelet examples

The convolution for a signal $x(t)$ in the time domain is defined as

$$T(A,B) = \int_{-\infty}^{\infty} x(t)\psi^*_{A,B}(t)dt \qquad (7)$$

where $\psi_{A,B}(t)$ is the normalized wavelet function[1] written as

$$\psi_{A,B}(t) = \frac{1}{\sqrt{A}}\psi\left(\frac{t-B}{A}\right) \qquad (8)$$

The parameter A is the dilation parameter and is used to scale (stretch or squeeze) the wavelet. The parameter B is used to translate (shift) the wavelet to various locations, see Figure 3.

The convolution of the signal with a set of scaled and translated wavelet functions generates a two dimensional transform plane as indicated in Figure 4. The x-axis represents the location (e.g. time shift) of the wavelet function while the y-axis indicates the current scale of the wavelet. This two dimensional representation of the signal shows the correlation between

[1]The symbol '*' indicates that the complex conjugate of a wavelet function is used in the transform, when using complex wavelet functions.

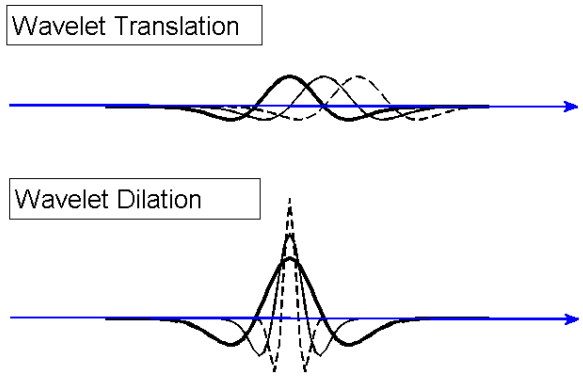

Figure 3: Wavelet translation and dilation

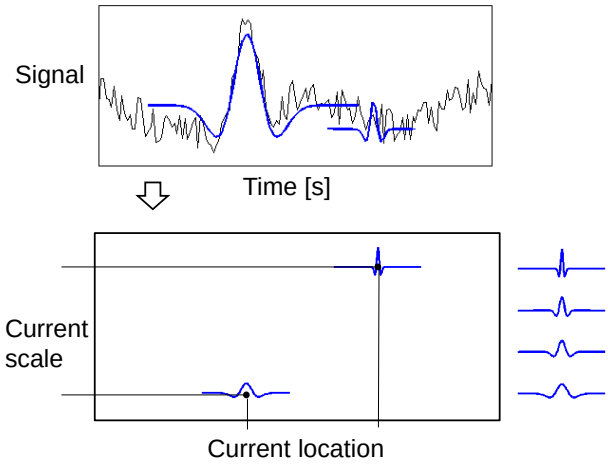

Figure 4: Two dimensional transform plane scheme

the wavelet and the signal. If the signal matches well with a wavelet at a certain position, a large value in the transform plane is expected.

Mallat [12] has shown that a multiresolution representation of the signal is achieved by applying the Discrete Wavelet Transform (DWT) using a set of parameters A and B.

The multiresolution representation transforms the signal into a combination of approximations and details coefficients, see Figure 5. The approximations contain the low frequency information and can be interpreted as general trend of the signal, whereas the details contain the higher frequency information. For the inverse operation, an original signal is quickly completely reconstructed, without loosing any information, using its approximation and its detail.

Another method to analyze discrete signals is the Wavelet Packet Transform (WPT). It is a generalization of the discrete wavelet transform,

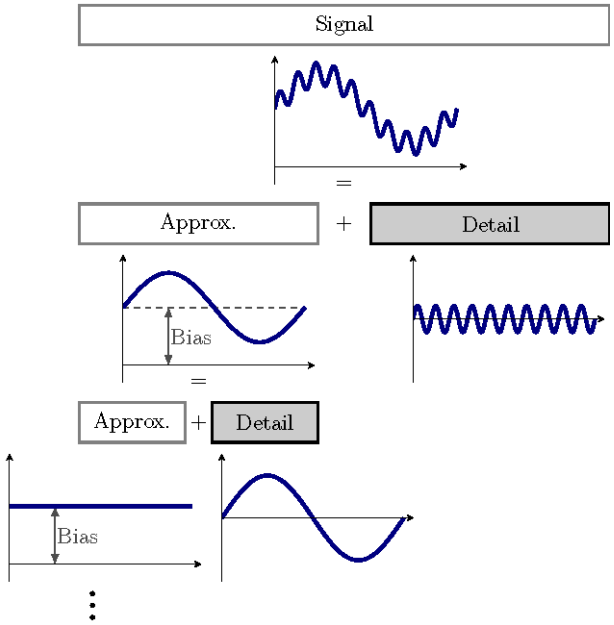

Figure 5: Multiresolution schematic representation from reference [14].

however herein the signal details and the approximations are further decomposed at each level. This method is extensively described in reference [13] and allows better resolution at higher frequencies creating a decomposition tree structure as seen in Figure 6.

Each level of decomposition in the WPT is represented by a Time-Frequency Plane (TFP) which is schematically depicted in the lower part of Figure 6. An example of such a visualization is shown in the lower plot of Figure 7, where a chirp signal is decomposed and represented by a TFP in natural frequency ordering. As expected, the frequency of the signal increases with increasing time (x-axis).

The decomposition coefficients are represented in the TFP's using so-called Heisenberg boxes. Each of this box defines the center frequency and location of the scaled and shifted wavelet function used to decompose the signal. In Figure 7 these Heisenberg boxes are represented by colored rectangles, where larger coefficients are plotted darker. This representation is similar to a spectrogram calculated from the time signal using the Fourier transform, where the frequency spectrum of a signal is depicted as it varies with time.

A time domain discrete signal can be reconstructed from the wavelet packet coefficients

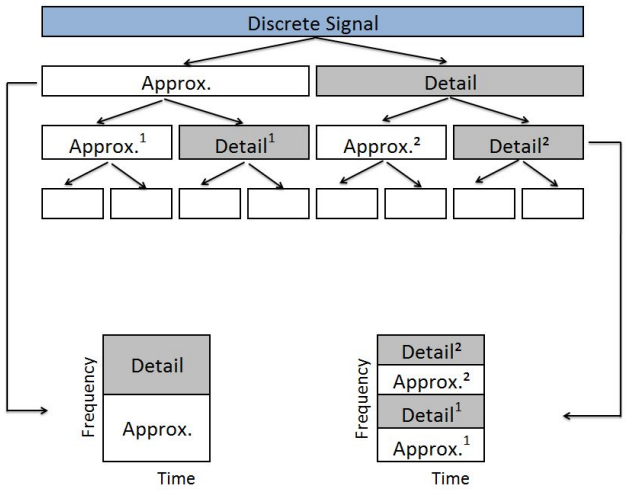

Figure 6: Wavelet packet transform

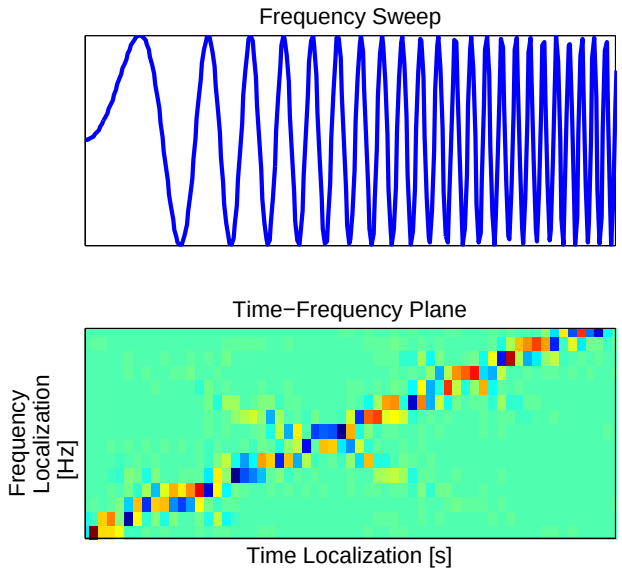

Figure 7: Frequency sweep decomposition

stored in the Heisenberg boxes of any admissible TFP. This preserves the time and frequency information for the signal. The methodology presented in the next section relies on this property to define control surface inputs with distinct frequency excitations at defined time localizations of the maneuver.

4 METHODOLOGY

The proposed maneuver design method is based on the idea of creating input signals which have distinct frequency band excitations at predefined maneuver times. An overview of the method is given in Figure 8.

Aircraft *a-priori* information is used to select

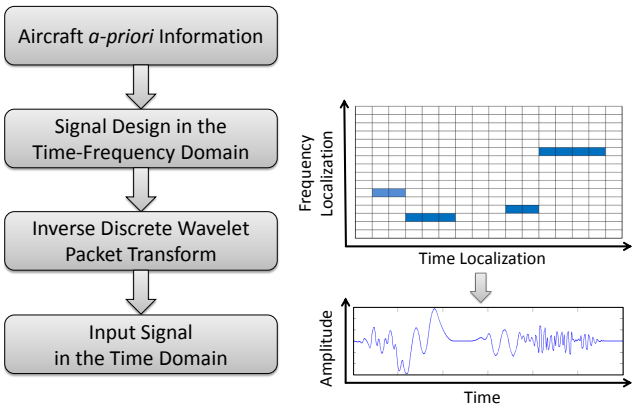

Figure 8: New input design method

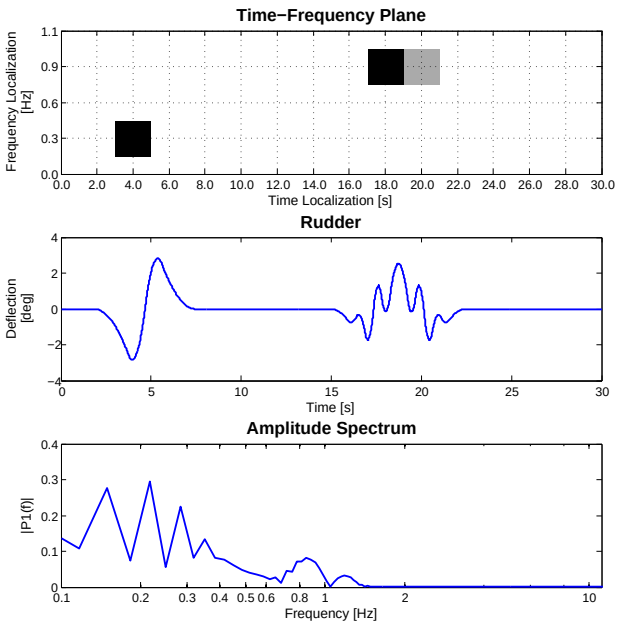

Figure 9: Rudder signal generation

the desired frequency band excitations for the signal. Heisenberg boxes in the TFP are used to represent this information in the time-frequency domain. An inverse discrete wavelet packet transform using a selected wavelet yields the desired signal in the time domain which can then be assigned to any of the control surfaces.

As will be shown in Section 4.2, this method also allows to define a single maneuver that uses several control surfaces at the same time. Through proper signal definition in the TFP, a time and frequency decorrelation between the different control inputs can be assured.

4.1 Single Input Using the Time-Frequency Plane

As the DWPT uses a dyadic scale the time-frequency plane must be defined as a square matrix having 2^{N_t} time segments and 2^{N_f} frequency segments. Each combination of a time segment and a frequency segment is a Heisenberg box. A value can be assigned to any of these Heisenberg boxes and the absolute value represents the local energy for the reconstructed signal, schematically depicted in Figure 9. Furthermore, due to the Inverse Discrete Wavelet Packet Transform (IDWPT), this value defines the amplitude of the input.

An example of a signal generation starting from values specified in a TFP definition is shown in Figure 9. The upper diagram of Figure 9 shows the TFP with 16 time segments and 16 frequency segments. The maneuver time was set to 30 seconds resulting in Heisenberg boxes with a width of 2 s and a height of 0.2753 Hz [2]. In this example an input with a frequency excitation in the 0.3 Hz band at 4 seconds and also a frequency content of 0.9 Hz at 18 to 20 seconds was specified by assigning values for the corresponding Heisenberg boxes. The generated signal is the direct result of the IDWPT and is shown in the center diagram of Figure 9. The lower diagram, shows the frequency content of the signal, evaluated by a fast Fourier Transform (FFT). This information can be used to evaluate if the combination of any wavelet chosen for the IDWPT introduces undesired frequencies for the aircraft excitation, e.g. elastic modes must not be excited during the rigid body dynamics identification.

4.2 Multi-Axis Maneuver Design

The multi-axis maneuver design method used in this work follows the same steps as for a single input described above. For each control surface a TFP is specified. To assess the correlation in time and frequency between different control surfaces an overlap diagram was created. It is a superposition between the TFP's of the selected input signals and gives a visual representation of the information used to define the inputs. Figure 10 shows the overlap diagram and

[2] In the time-frequency plane representations within this paper, the scale was rounded to one decimal place for visualization purpose

the resulting time histories for a combined rudder and aileron input maneuver. It is clearly visible that there is no concurrent frequency band excitation between these two control surfaces, even though both control surfaces are deflected simultaneously.

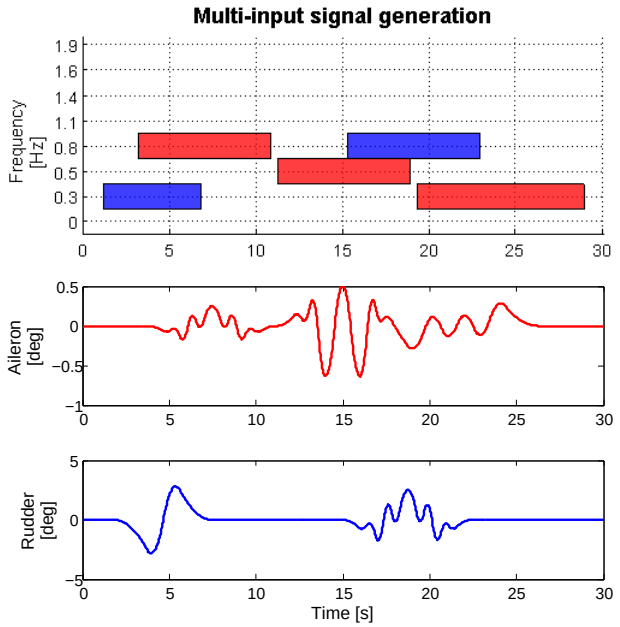

Figure 10: Multi-input signal generation scheme

5 SIMULATION AND RESULTS

Simulations with a high quality Airbus A320 dynamic model were used to obtain virtual flight test data. This model has been derived from an extensive flight test campaign during the DLR internal project OPIAM (Online Parameter Identification for Integrated Aerodynamic Modeling) and includes compressibility and ground effects, high alpha characteristics and meets the criteria for simulator validation and qualification [15].

Maneuvers using the new design method just described were first developed for the longitudinal motion, using only elevator and horizontal tail as control inputs. Therefore only the aerodynamic parameters of the longitudinal motion could be estimated from a subsequent estimation using this maneuver.

After this proved to be successful a multi-axis maneuvers using elevator, horizontal tail, aileron and rudder were designed to allow estimation of the full set of aerodynamic parameters. Compressibility, non-linear lift behavior and ground effect were neglected for all identification runs and the parameters were always assumed to be constant for the respective maneuver.

5.1 Longitudinal Motion

The method described in Section 4 was used to define a maneuver to identify the aircraft's aerodynamic parameters for the longitudinal motion. Two control surfaces were used for the maneuver: the elevator and the horizontal tail.

Inputs for the elevator contain high frequency excitations to evaluate the short period motion as well as low frequency excitations to obtain a phugoid-like response. The horizontal tail is being deflected simultaneously in order to estimate its characteristics and the downwash parameters. For the elevator a bior wavelet, as depicted in Figure 2, was chosen to generate a signal with no sharp edges.

In order counteract the deviation from the trim point, the horizontal tail is being deflected in the opposite way as the elevator. A variation of less than 1.5 degrees of angle of attack and of no more than 4% of true airspeed allows the estimation of parameters without any need to account for additional compressibility effects. Therefore, the aerodynamic parameters can be assumed constant throughout the complete maneuver at a given flight test point.

Figure 11 shows the input signal generated for the elevator. The upper diagram shows the definition of the time-frequency plane. A 16x16 TFP was chosen resulting in Heisenberg boxes with a width of 2 s and height of approximately 0.28 Hz. The center diagram shows the resulting signal from the inverse wavelet packet transform. The bottom diagram in Figure 11 shows the frequency content of the final signal. It can be seen that no high frequency is excited. This is desired when creating signals for rigid body identification. For the elastic modes, frequencies from 3 Hz and higher are generally expected. Thus, no elastic mode is expected to be considerably excited during this maneuver.

Usually some *a-priori* information for a new aircraft is available from wind tunnel results, CFD calculations or after the preliminary design. With the proposed design method, the expected natural frequencies can easily be excited b using corresponding frequency bands. In the current

evaluation, the expected short period natural frequency is 0.35 Hz. Therefore three frequency bands, centered at 0.28, 0.55 and 0.83 Hz, are included for the signal generation. For the phugoid mode, the expected natural frequency is much lower, in the order of 0.02 Hz. Therefore, a classical pulse is emulated using the lowest frequency band over a few time tilings. For display purposes, only relevant portions of the chosen time-frequency plane tilings are shown, meaning that all other coefficients are zero and do not influence the results of the IDWPT.

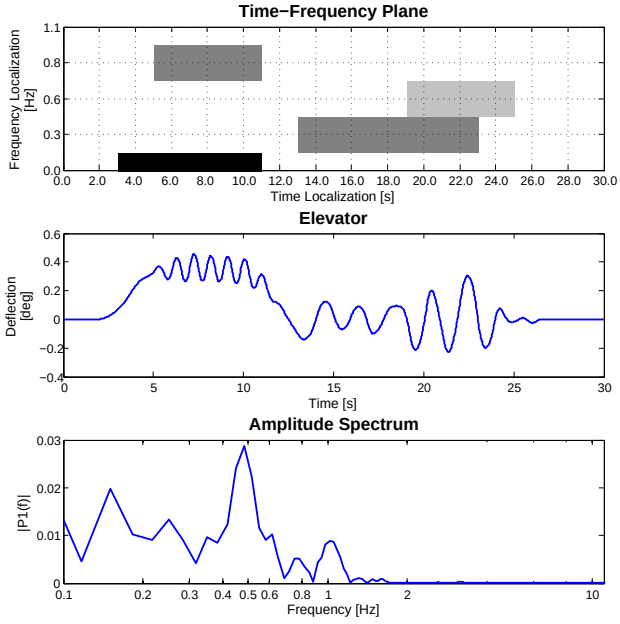

Figure 11: Elevator signal generation

Parameter estimation was performed using the output error method in the time domain and the aerodynamic model for a rigid body aircraft for the longitudinal motion as described by Equations (4) - (5).

The comparison between the simulated flight data and the identified longitudinal motion model are shown in Figure 12 and the results of the comparison of the time histories are given in Table 1. The maximum absolute difference between the identified model and the simulated flight test data is shown in the second column. The last column gives the relative difference to the overall output amplitude during the maneuver.

Identified parameters for the longitudinal motion are shown in Table 2. The relative difference between the true value from the simulation model and the estimated value for the reduced model is

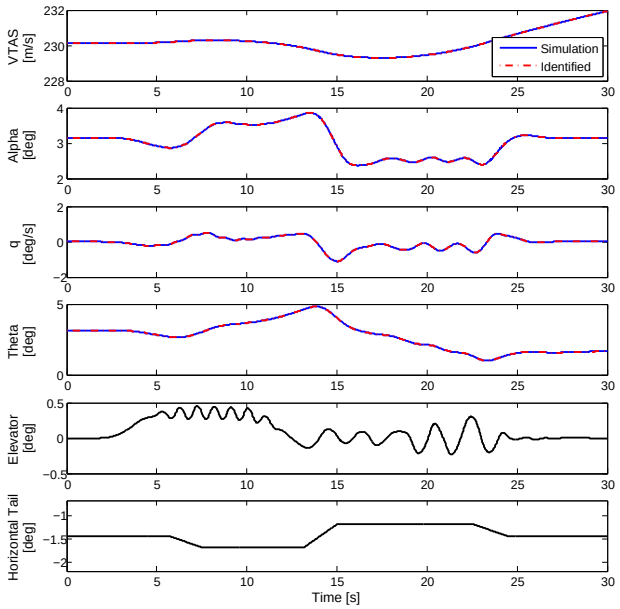

Figure 12: Time history comparison plot of simulated flight data (blue) and identified model outputs (red), with inputs for elevator and horizontal tail (black)

Output	max. diff.	Δ diff. [%]
V [m/s]	0.011	0.42
α [deg]	0.003	0.19
q [deg/s]	0.008	0.48
θ [deg]	0.019	0.50

Table 1: Comparison between simulated and identified models outputs for the longitudinal maneuver

given in the last column.

The lift parameters were obtained with highest accuracy, whereas the drag parameters are less accurate. This could be related to the fact that there is little speed variation during the maneuver, hence only a small portion of the drag polar is covered. Also $C_{L_{q,WB}}$ and $C_{m_{q,WB}}$ are of reduced accuracy, mainly because these contributions are small in relation to the pitch rate influences derived from the horizontal tail.

These results show that it was possible to design a maneuver using the method in Section 4 that allows to successfully identify 10 parameters that accurately describe the longitudinal motion for the rigid body aircraft, only using the *a-priori* information of desired frequencies and a proper wavelet function.

Parameter	True Value	Estimate	Δ [%]
C_{L_0}	0.245	0.245	-0.03
$\delta\varepsilon/\delta\alpha$	0.612	0.627	2.44
$C_{L_{q,WB}}$	3.734	3.968	6.28
$C_{L_{\alpha,WB}}$	5.281	5.322	0.76
$C_{L_{\alpha,HT}}$	4.445	4.437	-0.18
$C_{L_{\eta,HT}}$	1.733	1.736	0.14
C_{D_0}	0.021	0.018	-13.49
e	0.600	0.707	17.90
$C_{m_{0,WB}}$	-0.192	-0.193	0.49
$C_{m_{q,WB}}$	-7.591	-7.176	-5.46

Table 2: Parameter estimates for the longitudinal motion

5.2 Multi-Axis Maneuver

To be able to estimate the aerodynamic parameters for a complete aircraft model, a multi-axis maneuver was designed using elevator, aileron, rudder and horizontal tail as control inputs.

For the elevator and horizontal tail, the same input as in Section 5.1 were used.

The input signal generation for the other control surfaces is shown for the rudder in Figure 9 and for the aileron in Figure 13. The signal designs were performed using a 16x16 time-frequency tiling. This results in Heisenberg boxes with a width of 2 s and height of 0.28 Hz. The dutch roll of the aircraft is excited in the beginning of the maneuver by a rudder input with low frequency at approximately 0.28 Hz. Furthermore the aileron is deflected to get the roll motion excited. This is the same approach as for the classical maneuver design criteria, described in [4]. Additional high-frequency inputs are applied to the aileron at the beginning of the maneuver and to the rudder in the second half of the maneuver, shown in Figure 10. The signals generated for the control surfaces do not contain any high frequencies thus avoiding significant excitation of elastic modes.

Parameter estimation was again performed using the output error method in the time domain and the aerodynamic model for a rigid body aircraft as described with the complete set of Equations (4) - (5).

Overall, a multi-axis maneuver was successfully designed and allows the estimation of 21 aerodynamic parameters that describe the rigid

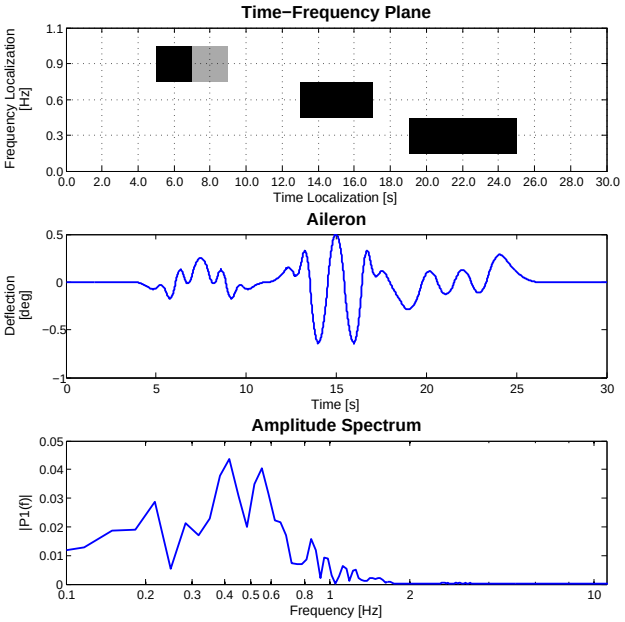

Figure 13: Aileron signal generation

body aircraft dynamics in six degrees of freedom. Plots for the longitudinal and lateral-directional motion of the aircraft can be seen in Figure 14. The comparison results between the outputs of the identified model and simulated flight test data is given in Table 3.

Output	max. diff.	Δ diff. [%]
V [m/s]	0.015	0.49
α [deg]	0.010	0.31
q [deg/s]	0.012	0.73
θ [deg]	0.027	0.70
β [deg]	0.048	0.72
p [deg/s]	0.021	0.66
r [deg/s]	0.063	0.65
ϕ [deg]	0.149	0.66

Table 3: Comparison between simulated and identified models outputs for the multi-axis maneuver

Table 4 shows that all main parameters are estimated with good accuracy. The rolling moment due to the aileron deflection (C_{l_ξ}) has low accuracy (high deviation to the true parameter) and the signal could be adjusted for a better estimation of this parameter. It should be emphasized, that analogous to the longitudinal maneuver, the model used for identification is a simplified model with some selected parameters to describe the

Parameter	True Value	Estimate	Δ [%]
C_{L_0}	0.245	0.246	0.42
$\delta\varepsilon/\delta\alpha$	0.612	0.635	3.68
$C_{L_{q,WB}}$	3.734	4.911	31.53
$C_{L_{\alpha,WB}}$	5.281	5.310	0.54
$C_{L_{\alpha,HT}}$	4.445	4.445	0.01
$C_{L_{\eta,HT}}$	1.733	1.736	0.19
C_{D_0}	0.021	0.018	-15.14
e	0.600	0.709	18.24
$C_{m_{0,WB}}$	-0.192	-0.194	1.08
$C_{m_{q,WB}}$	-7.591	-7.166	-5.60
C_{Y_β}	-1.055	-0.998	-5.38
C_{Y_ζ}	0.331	0.314	-4.98
C_{Y_p}	0.199	0.299	50.50
C_{l_β}	-0.419	-0.433	3.31
C_{l_ξ}	-0.165	-0.147	-10.69
C_{l_ζ}	0.084	0.084	-0.28
C_{l_p}	-0.901	-0.943	4.66
C_{l_r}	0.227	0.235	3.51
C_{n_β}	0.432	0.448	3.83
C_{n_ζ}	-0.325	-0.323	-0.54
C_{n_r}	-0.710	-0.630	-11.22

Table 4: Parameter estimates for the complete aircraft motion

longitudinal and lateral-directional motion. For instance there might be an angle-of-attack influence on the (C_{l_ξ}), namely ($C_{l_{\xi,\alpha}}$), which is not being identified, yielding the higher error in the (C_{l_ξ}) parameter. As for the longitudinal motion maneuver in Section 5.1 the drag parameters are less accurate due to small change in the speed for a drag polar estimation. Some second order derivatives such as C_{Y_p} and C_{n_r} are also estimated with low accuracy, however the comparison plots in Figure 14 show that a good match between simulated flight test data and identified model is obtained.

6 COMPARISON WITH OTHER MANEUVER DESIGN METHODS

The proposed methodology reuses an idea which can already be found in the literature, namely applying simultaneous uncorrelated inputs for system identification [6, 7, 16]. The fact that uncorrelated inputs are used permits to ensure that the effects of the respective inputs can be separated afterward. One possibility is to use sums of pure sine signals with disjointed sets of frequencies for each input. This strategy can be found in many textbooks, e.g. [16], and has been already used for airplane system identification, e.g. by Morelli [6].

Whilst the sum of sines type of signals allows elegant and very efficient parameter estimation in the frequency-domain, the comparison between the (real) aircraft reaction and the model based on such signals can hardly be interpreted by system identification specialists. Indeed, very often the correct model structure is not known beforehand and the system identification specialists need to adjust the model structure and must decide which parameters should be estimated.

Usually, a system identification specialist can perform a good diagnostic and know what needs to be changed in the model, just by comparing the real aircraft and model responses after exciting the aircraft with standard well known system identification maneuvers (e.g. pulses, doublets, 3211-inputs, frequency sweeps, etc.). The permanent excitations of different frequencies by a sum-of-sine signal make this diagnostic impracticable and thereby the ”expert-based” model improvement process impossible.

An automatized search for suitable model terms can be performed as proposed in [17, 18] but the search is then based on a series of terms which will not necessarily correspond to physically meaningful effects. For instance, by adding higher order terms from a polynomial basis any continuous nonlinear function can be approximated very well, but no physical interpretation can be made from a $C_{m,\alpha^3 q}$ or $C_{m,\alpha^3 \eta}$ term. Such high-order terms are not physically justified by a particular phenomenon but just an artificial mean to get a higher goodness of fit.

For this reason, the author and his research group prefer to stay in control of the model structure selection process and add terms only as needed and wherever adding a new term can be justified. In this context, having maneuvers to which the response of the system can be interpreted by a flight mechanics expert is more advantageous than having maneuvers that enable the use of a highly efficient parameter estimation formulation in the frequency-domain.

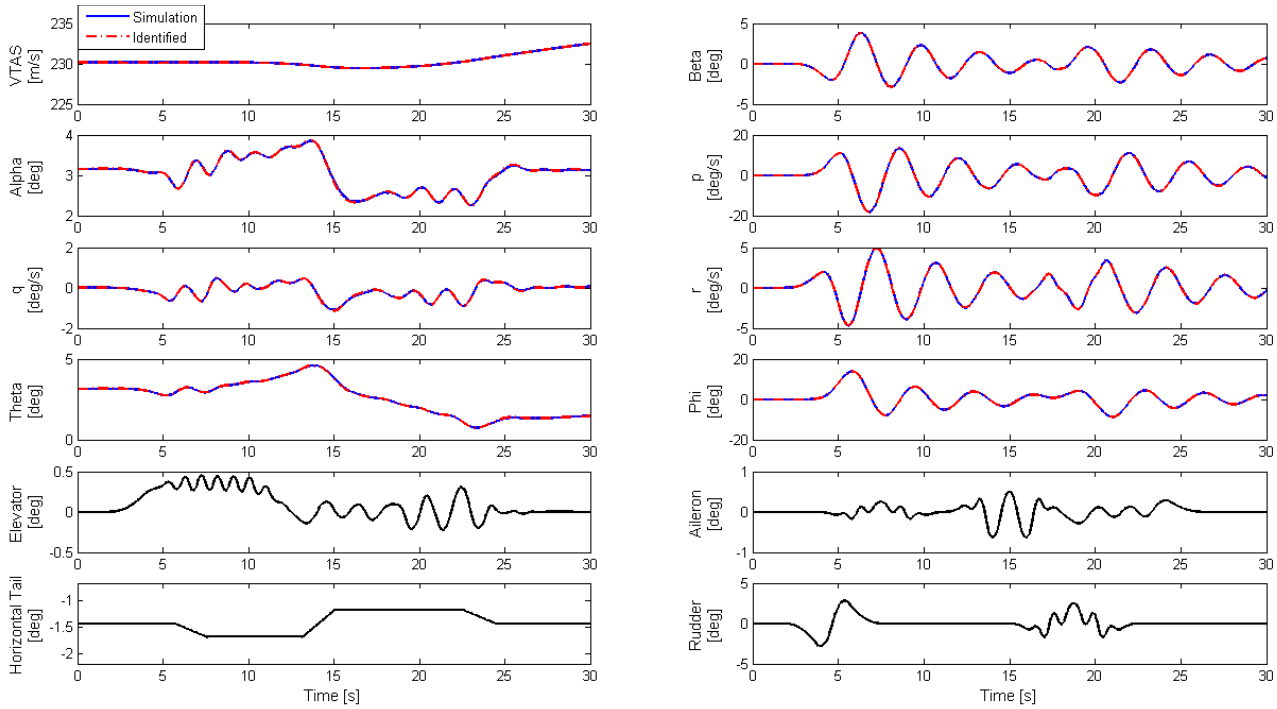

Figure 14: Response time histories from simulated flight test data (blue) and reduced model outputs (red), with multi-surface inputs (black)

7 CONCLUSION AND OUTLOOK

In this work, a new method to design single or multi-axis maneuvers for aircraft parameter estimation was presented and discussed. The proposed method permits to design single-axis and multi-axis excitation maneuvers suited for aircraft parameter estimation. Based on classical design criteria, the methodology developed allows the design of complex signals including *a-priori* information on the system to be identified (here the aircraft) even though only a quite restricted number of parameters is used to describe these signals.

The new method for maneuver design has shown promising results for both, single-axis and multi-axis excitations. Parameter estimates derived from virtual flight test data of maneuvers designed using the new method have shown that this design method can be applied to specify maneuvers with the potential to reduce flight test time, and further on to improve the quality of aerodynamic models. The proposed method was demonstrated based on a 30 second maneuver which permitted to successfully identify the aircraft aerodynamic parameters for the longitudinal motion. It was also successfully demonstrated that it was possible to design a 30 seconds maneuver for which 21 parameters describing the complete aircraft rigid body dynamics for a single flight test point were accurately estimated.

The proposed method can easily lead to very compact multi-axis maneuvers to which the response of the system will remain easily interpretable by a specialist. However, the resulting maneuvers may lead to less efficient parameter estimation than some of the alternatives when considering frequency-domain parameter estimation. Users will therefore have to choose based on the requirements of their application which approach is preferable.

The high level parameters provided, especially type of wavelets and scale, seem very well suited for further automatic optimization of the maneuvers aiming at maximizing the quality of the identified parameters. Whilst such an optimization remains a medium-term goal at this stage of the development, it should be noticed that the parametrization used herein will ease the interpretation of the parameter values that would be obtained through the optimizer. The other way around, the *a-priori* knowledge available on the system can easily be included in the design of the signal in order to be certain to excite the rele-

vant dynamic modes of the system.

The proposed methodology also permits to design signals very quickly, not only rich in information content, but also satisfying very specific constraints, which can be fully or almost fully uncorrelated.

Work on the presented methodology will be pursued for optimizing multi-axis maneuvers of virtual flight tests for system identification of flexible aircraft (DLR project VicToria [19]) as well as for optimization of flight test campaigns for system identification.

References

[1] Marchand, M.: *Untersuchung der Bestimmbarkeit von Flugzeugderivativen aus Flugversuchen*. Technical Report DLR-IB 154-74/32, DLR Institut für Flugsystemtechnik, 1974.

[2] Marchand, M.: *Untersuchung der Bestimmbarkeit der flugmechanischen Derivative des CCV-Versuchsträgers F-104 G*. Technical Report DLR-IB 154-77/12, DLR Institut für Flugsystemtechnik, 1977.

[3] Plaetschke, E. and Schulz, G.: *Practial Input Signal Design*. AGARD Lecture Series No. 104 - Parameter Identification - Paper 3, 1979.

[4] Jategaonkar, Ravindra V.: *Flight Vehicle System Identification*, volume 216 of *Progress in Astronautics and Aeronautics*. American Institute of Aeronautics and Astronautics, Inc., 1801 Alexander Bell Drive, Reston, VA 20191, 2006.

[5] Wells, W. and Ramachandran, S.: *Multiple Control Input Design for Identification of Light Aircraft*. IEEE Transactions on Automatic Control, Vol 22, No. 6, 985-987, 1977.

[6] Morelli, Eugene A.: *Multiple input design for real-time parameter estimation in the frequency domain*. IFAC Proceedings Volumes, Vol. 36, No. 16, page 639 – 644, 2003. 13th IFAC Symposium on System Identification (SYSID 2003), Rotterdam, The Netherlands, 27-29 August, 2003.

[7] Morelli, Eugene A.: *Flight Test Maneuvers for Efficient Aerodynamic Modeling*. Journal of Aircraft, Vol. 49, No. 6, page 1857–1867, November 2012.

[8] Lichota, Piotr and Ohme, Per: *Design and Analysis of new Multi Axis Input Manoeuvres for Aircraft Sys-ID*. Technical Report DLR-IB 111-2014/46, DLR Institut für Flugsystemtechnik, 2014.

[9] Addison, P.S.: *The Illustrated Wavelet Transform Handbook: Introductory Theory and Applications in Science, Engineering, Medicine and Finance, Second Edition*. CRC Press, 2017.

[10] Raab, C.: *Aerodynamikmodell für das Forschungsflugzeug A320 ATRA*. Technical Report DLR-IB 111-2010/45, DLR Institut für Flugsystemtechnik, 2010.

[11] Mönnich, W.: *Ein 2-Punkt-Aerodynamikmodell für die Identifizierung*. Technical Report, Symposium 'Systemidentifizierung in der Fahrzeugdynamik'. DFVLR Mitteilung 87-22, Paper No. 3.1, 1987.

[12] Mallat, S.: *A Wavelet Tour of Signal Processing: The Sparse Way, Third Edition*. Elsevier Science, 2008.

[13] Jensen, A. and Cour-Harbo, A.: *Ripples in Mathematics: The Discrete Wavelet Transform*. Springer Berlin Heidelberg, 2001.

[14] Deiler, Christoph: *Data parser approaches for (online) parameter estimation*. CEAS Aeronautical Journal, Mai 2014.

[15] Raab, Christian: *A320-ATRA Flight Data Gathering for System Identification - 2nd Edition*. Technical Report DLR-IB-FT-BS-2016-354, DLR Institut für Flugsystemtechnik, Dezember 2016.

[16] Godfrey, K.: *Perturbation signals for system identification*. Prentice Hall international series in acoustics, speech, and signal processing. Prentice Hall, 1993.

[17] Morelli, Eugene A.: *Global nonlinear aerodynamic modeling using multivariate orthogonal functions*. Journal of Aircraft, Vol. 32, No. 2, page 270–277, July 1995.

[18] Grauer, Jared A. and Morelli, Eugene A.: *Generic Global Aerodynamic Model for Aircraft*. Journal of Aircraft, Vol. 52, No. 1, page 13–20, July 2015.

[19] DLR: *Project Victoria - Virtual Aircraft Technology Integration Patform*. Https://www.dlr.de/as/en/desktopdefault.aspx/tabid-11460/20078_read-47033/, August 2018.